

GNSS Satellite Observations with Interference Measurement Technology

Li Li, Geshi Tang, Tianpeng Ren, Jing Sun, Ming Shi
and Junwei Wang

Abstract Interference measurement Technology has been proved as a very good space geodetic technique used to determine the Earth Orientation Parameters (EOP), the Terrestrial Reference Frame (TRF), and the Celestial Reference Frame (CRF). For the rigorous determination of the entire system of TRF-EOP-CRF, there is an urgent need for alternative methods for connecting various spatial geodetic techniques. Using Very Long Baseline Interferometry (VLBI) to observe the GNSS satellites is a promising solution. This paper analyzes the importance and key issues of GNSS satellite observations with Interference measurement technology. This work studies the tracking of interferometric measurements of GEO satellites, tracks the Beidou satellite to verify the tracking measurement technology, and obtains the time-delay measurement of ns level. The orbit determination is completed by processing the measured data, we use single baseline and double baseline data for the orbit determination. The maximum orbit deviation of the single—baseline orbit determination is nearly 40 km, the accuracy of the orbit determination is significantly improved by using the double baseline data. The maximum orbital deviation is less than 1.5 km.

Keywords Interference measurement · Time delay · BeiDou

1 Introduction

Very Long Baseline Interferometry (VLBI) is a well-probed space geodetic technique used to determine the Celestial Reference Frame (CRF), the Terrestrial Interpretation and comparison of geodetic measurements have to be made in one common reference system in order to achieve correct and reliable results. In geodetic practice, coordinates are usually provided either in the kinematical International Terrestrial Reference Frame (ITRF) or in the quasi-inertial

L. Li (✉) · G. Tang · T. Ren · J. Sun · M. Shi · J. Wang
Beijing Aerospace Control Center, Beijing 100094, China
e-mail: lynnsee720@163.com; 13810205290@163.com

© Springer Nature Singapore Pte Ltd. 2017
J. Sun et al. (eds.), *China Satellite Navigation Conference (CSNC) 2017
Proceedings: Volume III*, Lecture Notes in Electrical Engineering 439,
DOI 10.1007/978-981-10-4594-3_10

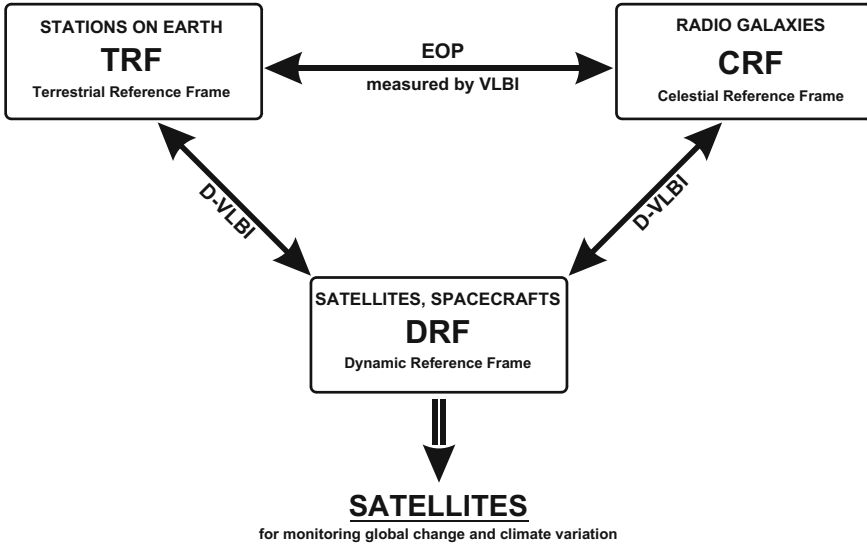


Fig. 1 The importance of reference frames for monitoring global change and climate variation

International Celestial Reference Frame (ICRF), whereas measurements of space probes such as satellites, spacecrafts, or planetary ephemerides rest upon dynamical theories. To avoid inconsistencies and errors during measurement and calculation procedures, exact frame ties between kinematic and dynamic reference frames have to be secured. By observing space probes alternately to radio sources with the differential Very Long Baseline Interferometry (D-VLBI) method, the relative position of the targets to each other can be determined. As the positions of the radio sources are well known in the ICRF, it is possible with such observational configurations to link the bodies of the solar system with the ICRF. While the Earth Orientation Parameters (EOP), which are regularly provided by the International Earth Rotation and Reference Systems Service (IERS) link the ICRF to the ITRF, the ties between the terrestrial and the dynamic frames will be established by D-VLBI observations (Fig. 1).

2 Observations to BeiDou Satellite

2.1 Purpose of the Observation

We use a single baseline interferometric system to track the calibration satellite and the satellite to be measured. The equipment delay, clock error of the equipment is obtained by the calibration satellite. The geometrical delay of the measured satellite is obtained by deducting the equipment delay of the measured satellite from the

interferometric delay. The geometric time delay is used as the orbit determination input to complete the orbit determination.

We take the Beidou GEO satellite C03 (110.5 E) as a calibration satellite, Beidou GEO satellite C02 (80E) as the measured satellite, as shown in Fig. 2.

The observation is based on the interference measurement system composed of two antennas of HangTianCheng and Changping Shahe. The baseline length is about 5.5 km. The observation plan is:

- Phase1: Day1, 22:00:00 start to observe the calibration satellite C03, for 2 h
- Phase2: Day2, 03:10:00 start to observe the measured satellite C02, for 8 h
- Phase3: Day2, 13:20:00 start to observe the calibration satellite C03, for 2 h

Because the interference baseline is short, the ionosphere and neutral atmosphere delay of the same target signal arriving at different station propagation paths are basically the same, so the propagation delay is not considered. The theoretical geometric time delay is obtained by using C03 precision ephemeris, and the difference between C03 interferometric measurement delay and theoretical geometric time delay is taken as device delay. The C02 geometry delay is deducted from the C02 interferometric measurement delay and the device delay. The geometric time delay of C02 is taken as the input of orbit determination, and the solution ephemeris is obtained.

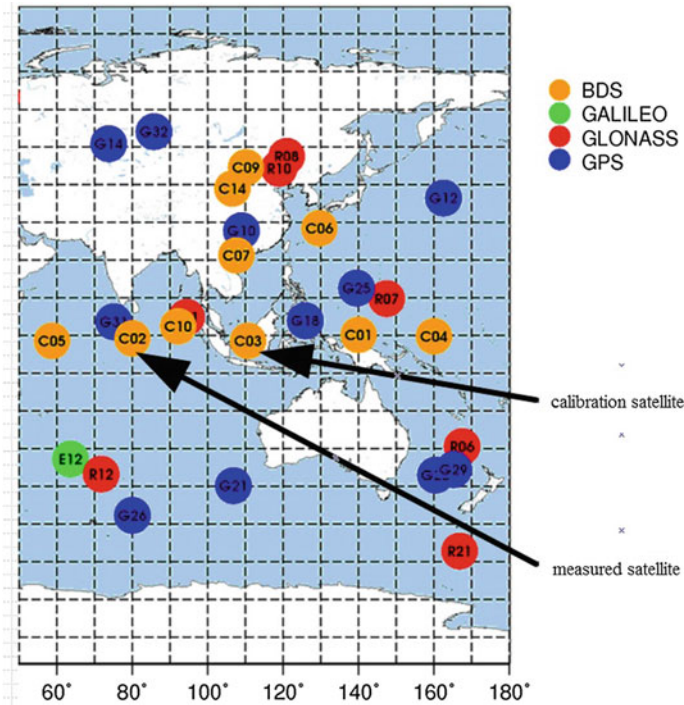


Fig. 2 Targets of the differential interferometry observation

After the observation, the theoretical geometric time delay can be obtained by C02 precise ephemeris, and the difference between the theoretical geometric time delay and the actual geometric time delay is regarded as the measurement precision. The difference between the solution ephemeris of C02 and the precision ephemeris is regarded as the orbit determination precision.

2.2 Satellite Signal Spectrum

In the observation, the spectrum of C03 and C02 downlink signals collected by the interferometric system are shown in Fig. 4. The signal with a higher signal-to-noise ratio is selected as the interference object. (As shown in “o” in Fig. 3a and “+” in Fig. 3b). Interference bandwidth is about 250 kHz. The interference fringe is obtained as shown in Fig. 4.

2.3 Analysis of Interference Delay and Error

We interfered with the original data of C03 and C02 collected by interferometric system, and the integration time is 2 s. We obtain the group delay, phase delay and theoretical geometric delay based on the precise ephemeris of C03 in observation

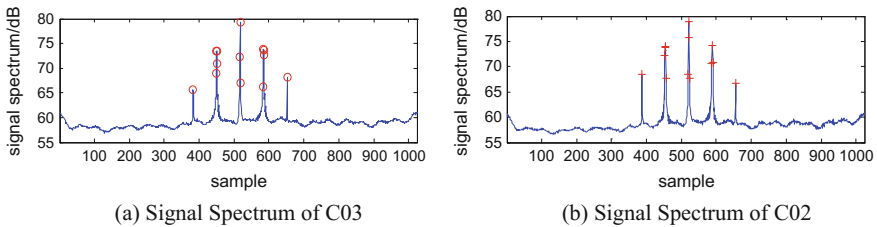


Fig. 3 Downlink signal spectrum of Beidou satellite C03 and C02 (Sampling rate, $f_s = 1.0$ MHz)

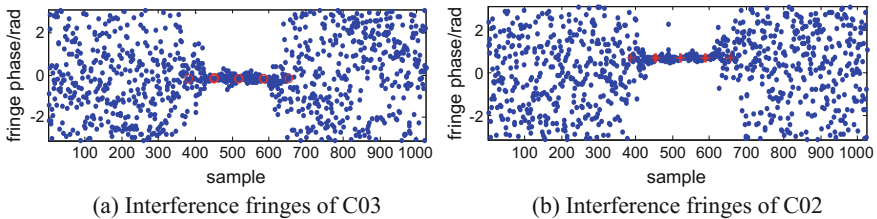


Fig. 4 Interference fringes of Beidou satellite C03 and C02 (Sampling rate, $f_s = 1.0$ MHz)

phase 1 and observation phase 3, and take the phase delay as the interference measurement delay, as shown in Fig. 5.

We obtain the group delay and phase delay of C02 in observation phase 2, where the group delay measurement noise is about 4.01 ns (the residual effective value of the group delay minus the phase delay), the phase delay measurement noise is about 9.4 ps (a 300-second linear fit residual RMS value). We consider the phase delay as the interferometric delay, as shown in Fig. 6.

We use the C03 interferometric measurement delay to subtract its theoretical geometric delay to obtain the interferometric measurement device delay during the C03 observation period. We linearly interpolate the device delays of observation phase 1 and observation phase 3 to obtain the interpolation device delay of

Fig. 5 Interference delay and theoretical geometric delay of C03

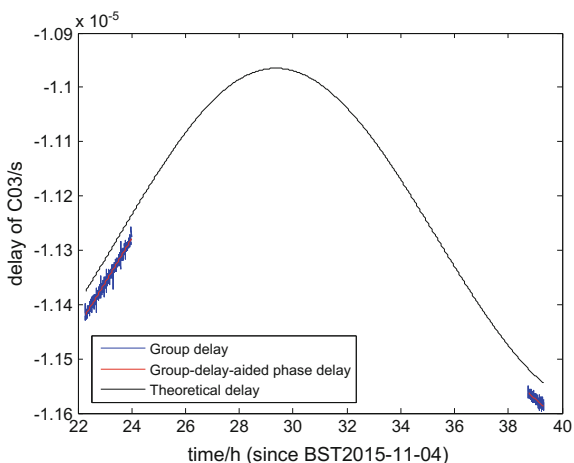
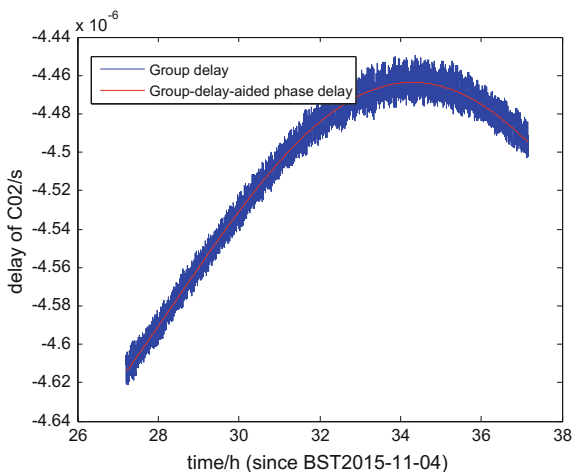


Fig. 6 The interferometric delay of C02



observation phase 2 for calibrating the measurement results of C02, as shown in Fig. 7. We subtract the interpolated device delay from the interferometric measurement delay of C02 in the observation phase 2 to obtain the geometric time delay of C02 for subsequent trajectory determination.

To estimate the interferometric error (ie, the difference between the geometric delay of C02 and the theoretical geometric time delay), the theoretical geometric time delay is derived using the C02 precision ephemeris, as shown in Fig. 8. It can be seen that the interferometric error is about 0.267 ns (rms) and 0.536 ns (max).

Fig. 7 Device delay, and interpolation device latency of C03

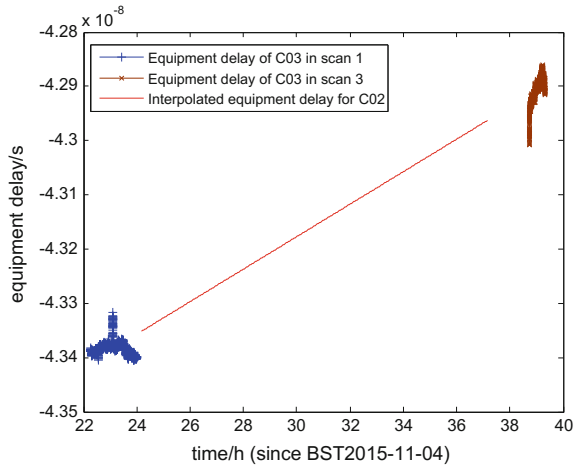
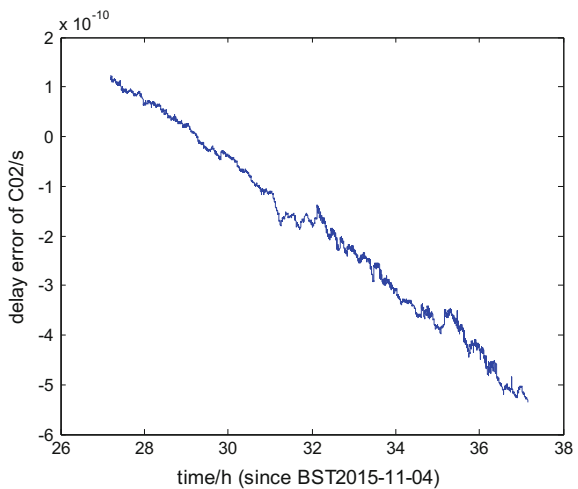


Fig. 8 Interference measurement error of C02



2.4 The Result and Accuracy of Orbit Determines

The interpolation delay is subtracted equipment delay from the C02 interferometric measurement delay to obtain the geometric time delay as the input to the orbit determination solution. The resolution of ephemeris is compared with the precision ephemeris to evaluate the orbit determination accuracy.

After solving, the orbit determination based on C02 geometric delay is convergent. Figure 9 shows the comparison between the calculated trajectories and the precision ephemeris. It can be seen that the maximum error of the calculated trajectory in the X, Y, and Z directions in the CGCS2000 coordinate system is 26.8 km (shown as Fig. 9a), 12.4 km (shown as Fig. 9b), 23.5 km (shown as Fig. 9c). The orbital accuracy is limited due to single baseline measurements, if double baselines are used for measurement, the orbital precision will be greatly improved.

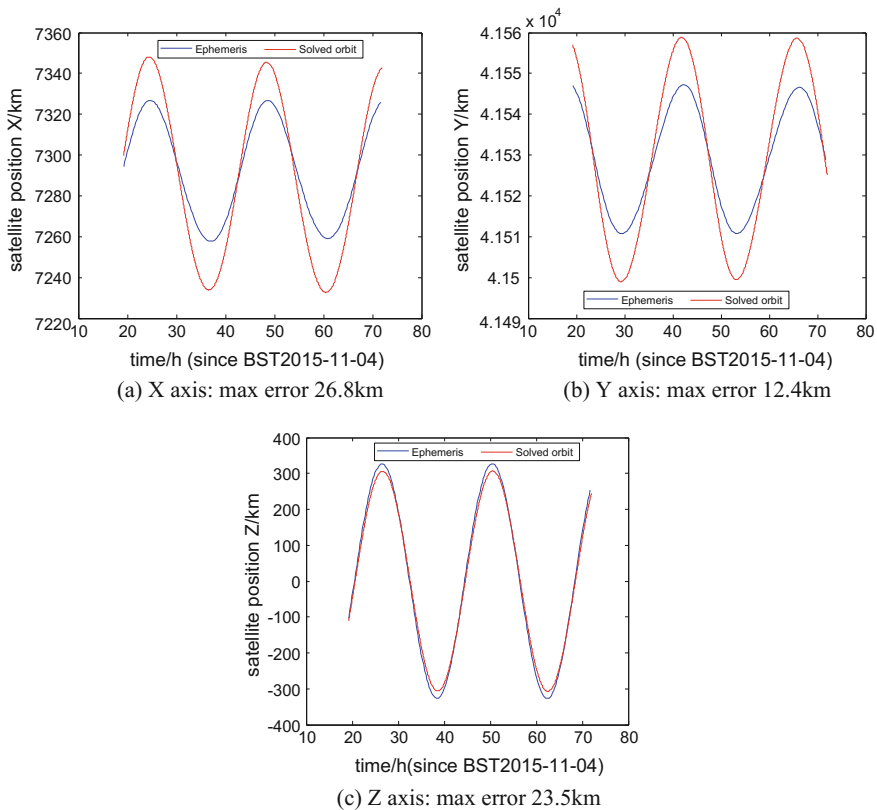


Fig. 9 Determination of GEO satellite orbit based on single baseline interferometry

2.5 Simulation of Double Baseline Data

Taking into account the current conditions cannot be achieved fiber optic connection dual baseline test, the use of simulation analysis for orbital calculation. Specific steps are: (1) The ephemeris integration is performed using the initial orbits as the benchmark for the validation of orbit determination. (2) The observed data are simulated using the reference orbit and the extracted data errors are added to the simulated data as the observed data. (3) Based on the simulation observed data, orbit determination is performed using single baseline and double baseline, and compare the orbit determination accuracy.

Initial simulation orbit:

Initial orbit epoch: 2016 10 01 00 00 00.000 (UTC)

Initial position:

41846493.638676	-5085894.663318	-116157.996570
370.374555	3053.016449	-1.853515

Orbit Determination of Single Baseline

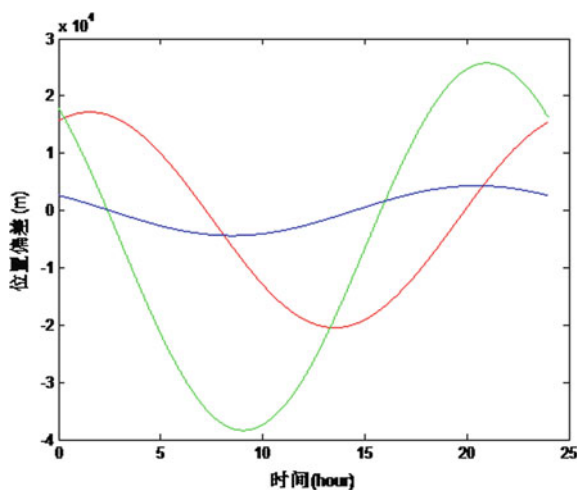
See Figs. 10 and 11.

Orbit Determination of Double Baseline

See Figs 12 and 13.

We use single baseline and double baseline data for the orbit determination. The maximum orbit deviation of the single—baseline orbit determination is nearly 40 km, the accuracy of the orbit determination is significantly improved by using the double baseline data. The maximum orbital deviation is less than 1.5 km.

Fig. 10 Deviation of orbit determination



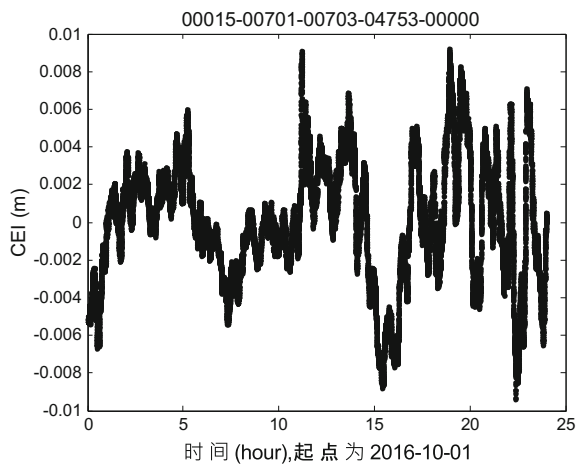


Fig. 11 Residuals of orbit determination

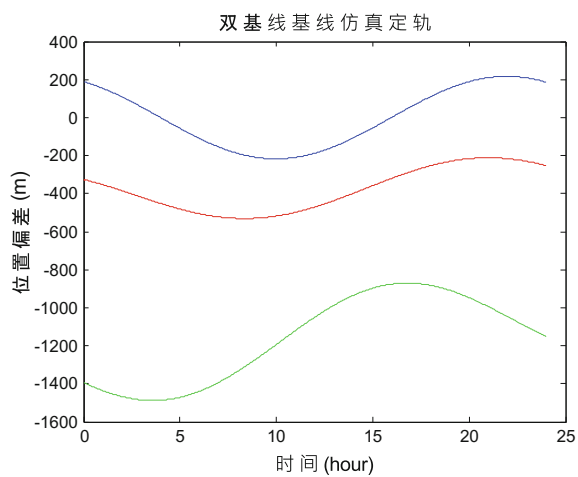


Fig. 12 Deviation of orbit determination

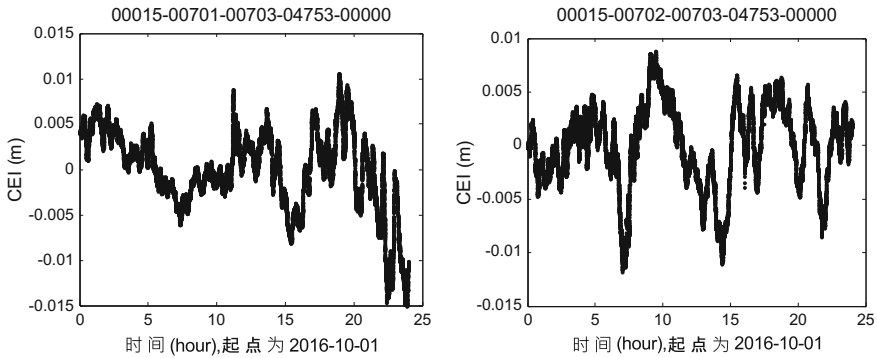


Fig. 13 Residuals of Orbit determination

3 Conclusions

Simulation results show that the double baseline tracking satellite is not only beneficial to the improvement of accuracy, but also can reduce the required observation arc length. The orbit accuracy of the order of 1 km can be achieved by approximately 6 h observation. Thus, the orbit accuracy of this tracking experiment is largely limited by the single baseline constraint. If double baseline tracking is used, orbit accuracy will be greatly improved.

Based on the short baseline interferometry system tracking GNSS satellites, is the first attempt of the county, this test successfully obtains the measurement data and the solution track. Although the data obtained in this experiment have certain systematic deviation, the accuracy of orbit determination is restricted, but this systematic deviations can be calibrated by other technical means. Therefore, we believe that this test has good engineering significance and application prospects.

Acknowledgements This work is sponsored by the National Natural Science Foundation of China (No. 11403001).

References

1. Briess K, Konemann G, Wickert J (2009) MicroGEM – microsattellites for GNSS earth monitoring, Abschlussbericht Phase 0/A. 15. September 2009, Helmholtz-Zentrum Potsdam Deutsches GeoForschungsZentrum GFZ and Technische Universität Berlin
2. CCSDS (2011) Delta-differential one way ranging (Delta-DOR) operations. Recommendation for space data system practices, Magenta Book, CCSDS 506.0-M-1-
3. King RW, Counselman CC, Shapiro II (1976) Lunar dynamics and selenodesy: results from analysis of vlbi and laser data. *J Geoph Res* 84(35):6251–6256
4. Sekido M, Fukushima T (2006) A VLBI delay model for radio sources at a finite distance. *J Geod* 80:137–149

5. Tornatore V, Haas R, Maccaferri G, Casey S, Pogrebenko SV, Molera G, Duvé D (2010) Tracking of GLONASS satellites by VLBI radio telescopes
6. Lambert SB, Poncin-Lafitte CL (2011) Improved determination of γ by VLBI (Research Note). *Astron Astrophys* 529:A70
7. Moyer TD (2003) Formulation for observed and computed values of deep space network data types for navigation. In: Yuen JH (ed) *JPL JPL deep space communications and navigation series*, Wiley, ISBN: 0-471-44535-5
8. Plank L (2013) VLBI satellite tracking for the realization of frame ties. PhD thesis
9. Li P, Hu X, Huang Y, Wang G, Jiang D, Zhang X, Cao J, Xin N (2012) Orbit determination for Chang'E-2 lunar probe and evaluation of lunar gravity models. *Sci China – Phys Mech Astron* 55:222–514
10. Sun J (2013) VLBI scheduling strategies with respect to VLBI2010. ISSN 1811–8380